A Sm(II)-Mediated Cascade Approach to Dibenzoindolo[3,2-b]carbazoles: Synthesis and Evaluation

Matthew T. Levick,[†] Iain Grace,[‡] Sheng-Yao Dai,[†] Nicholas Kasch,[§] Christopher Muryn,[†] Colin Lambert,[‡] Michael L. Turner,*[,†] and David J. Procter*[,†]
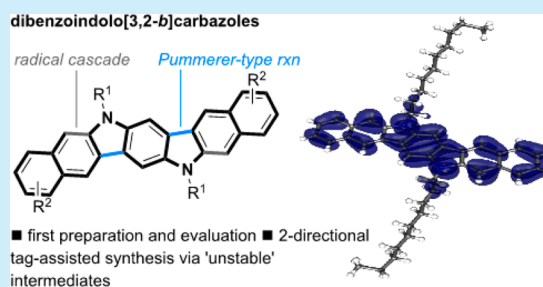
[†]School of Chemistry, University of Manchester, Oxford Road, Manchester, M13 9PL, U.K.
[‡]Department of Physics, Lancaster University, Lancaster, LA1 4YB, U.K.
[§]School of Physics and Astronomy, University of Manchester, Manchester, M13 9PL, U.K.

Ⓢ Supporting Information

ABSTRACT: Previously unstudied dibenzoindolo[3,2-b]carbazoles have been prepared by two-directional, phase tag-assisted synthesis utilizing a connective-Pummerer cyclization and a SmI_2-mediated tag cleavage−cyclization cascade. The use of a phase tag allows us to exploit unstable intermediates that would otherwise need to be avoided. The novel materials were characterized by X-ray, cyclic voltammetry, UV−vis spectroscopy, TGA, and DSC. Preliminary studies on the performance of OFET devices are also described.
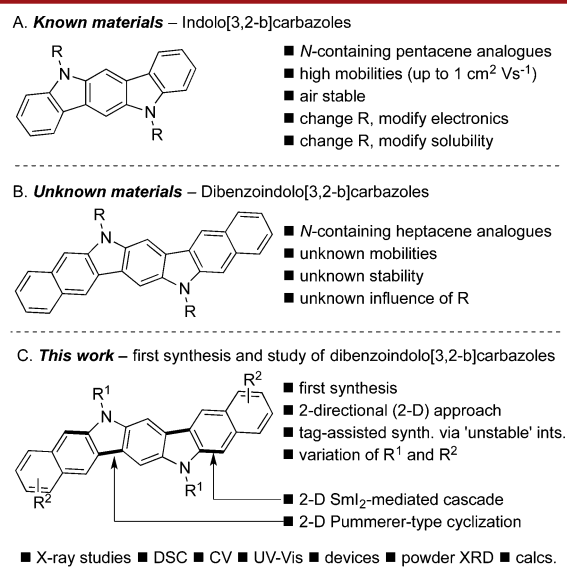
dibenzoindolo[3,2-b]carbazoles

radical cascade   *Pummerer-type rxn*

■ first preparation and evaluation ■ 2-directional tag-assisted synthesis via 'unstable' intermediates

Indolo[3,2-b]carbazoles, nitrogen containing analogues of pentacene, have been shown to be promising organic semiconductors with mobilities as high as 1 cm^2 V s^{-1}, with the advantage that the nitrogen atom allows for easy structural modification either to alter electronic properties or enhance solubility allowing for solution processing of devices (Figure 1A).[1] Larger acenes beyond pentacene are less well studied owing to the decreased stability as the conjugation length is increased.[2] Various methods have been employed to enhance the stability of the larger acenes to allow for a more detailed study of their properties, mainly via either extensive functionalization of the aromatic core or the inclusion of heteroatoms such as sulfur or nitrogen into the structure.[3] Herein we describe the synthesis, optical and electrochemical properties, and preliminary transistor performances of dibenzo-indolo[3,2-b]carbazoles [**DBICs**], a previously unknown class of aza-heptacenes based on an extended indolo[3,2-b]carbazole framework (Figure 1B). The first synthesis of **DBICs** involves the utilization of a two-directional Pummerer[4]-type cyclization and a two-directional radical cascade mediated by SmI_2.[5] Crucially, these two key steps incorporate the introduction and removal of a phase tag that facilitates the purification of unstable intermediates that would otherwise have to be avoided. Attractively, the use of tag introduction/cyclization and tag cleavage/cyclization[6] delivers a route in which the use of a phase tag adds no strategically redundant steps to the synthesis.

We have previously employed Pummerer-type cyclizations[7] in the synthesis of a range of different targets including bis-oxindole-based monomers for use in semiconducting poly-mers,[8] and benzo[b]carbazole end-capped oligothiophenes for preliminary evaluation as semiconductors.[9] Here we report an extension of this methodology in the first synthesis of dibenzoindolo[3,2-b]carbazoles.

Bis-hydroxyamides **1**, synthesized according to previously described procedures,[6,7] underwent oxidation and selective double Pummerer-type cyclization upon capture of a fluorous


A. **Known materials** – Indolo[3,2-b]carbazoles
■ *N*-containing pentacene analogues
■ high mobilities (up to 1 cm^2 Vs^{-1})
■ air stable
■ change R, modify electronics
■ change R, modify solubility

B. **Unknown materials** – Dibenzoindolo[3,2-b]carbazoles
■ *N*-containing heptacene analogues
■ unknown mobilities
■ unknown stability
■ unknown influence of R

C. **This work** – first synthesis and study of dibenzoindolo[3,2-b]carbazoles
■ first synthesis
■ 2-directional (2-D) approach
■ tag-assisted synth. via 'unstable' ints.
■ variation of R^1 and R^2
■ 2-D SmI_2-mediated cascade
■ 2-D Pummerer-type cyclization

■ X-ray studies ■ DSC ■ CV ■ UV-Vis ■ devices ■ powder XRD ■ calcs.

Figure 1. (A) Indolo[3,2-b]carbazole motif in organic semiconductors. (B) Unknown dibenzoindolo[3,2-b]carbazole (DBIC) motif. (C) This study: 2-D, tag-assisted synthesis and study of DBICs.

thiol $HS(CH_2)_2(CF_2)_7CF_3$ to give linear regioisomers (>5:1) **2** as a 1:1 mixture of diastereoisomers after rapid purification by fluorous[10] solid phase extraction (FSPE)[11] (Scheme 1).

Scheme 1. Two Directional, Tag-Assisted Synthesis of DBICs[a]
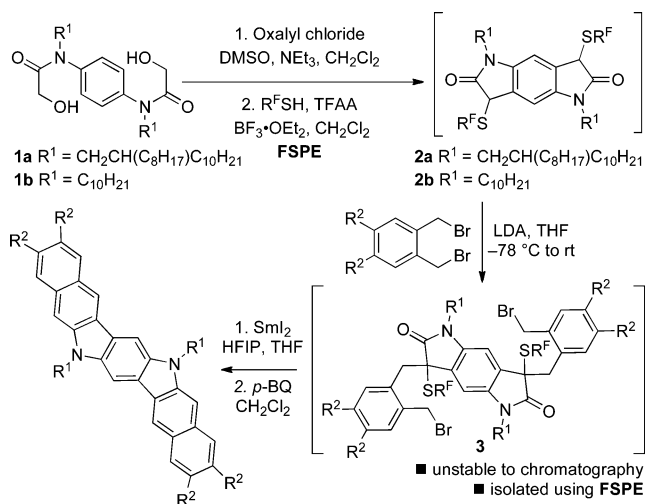
DBIC-1 $R^1 = CH_2CH(C_8H_{17})C_{10}H_{21}$, $R^2 = H$, 17% (5 steps from **1**; step av. 70%)
DBIC-2 $R^1 = C_{10}H_{21}$, $R^2 = H$, 16% (5 steps from **1**; step av. 69%)
DBIC-3 $R^1 = C_{10}H_{21}$, $R^2 = Me$, 10% (5 steps from **1**; step av. 63%)

[a]$R^F = -CH_2CH_2C_8F_{17}$. FSPE = fluorous solid phase extraction. HFIP = 1,1,1,3,3,3-hexafluoro-2-propanol.

Deprotonation and alkylation of **2** using LDA and a dibromo-alkylating agent gave key intermediates **3** that proved highly unstable toward conventional chromatography. Fortunately, purification by FSPE (rapid filtration through fluorous silica gel, eluting with a fluorophilic solvent) gave **3** with little decomposition. Finally, treatment of **3** with SmI_2 and a proton source at 60 °C triggered cleavage[12] of both fluorous tags and a double cyclization to give the desired **DBICs** after oxidation of the product mixture with p-benzoquinone (p-BQ). The novel aza-heptacenes were obtained in overall yields of 10−17% in 5 steps (average yield/step, 63−70%) from known and readily accessible hydroxyamides **1** (Scheme 1).

Slow evaporation from THF delivered crystals of **DBIC-2** and **DBIC-3** suitable for X-ray crystallographic analysis (Figure 2).[13] **DBIC-2** was found to pack in a lamellar-type structure (with the aromatic cores arranged in layers separated by regions of aggregated alkyl chains with an interlamellar spacing of 15 Å) in which the aromatic cores pack in a herringbone-like manner similar to pentacene but offset along the long axis of the molecule such that only three rings from each molecule are overlapping in the edge-to-face orientation. Each molecule is surrounded by six others via a shortest carbon−carbon distance of 3.5 Å, two in a completely offset parallel face-to-face arrangement and four in an edge-to-face manner.

DBIC-3 was found to pack in a herringbone motif, and segregation of the alkyl chains is again observed with an interlayer spacing of 16 Å (Figure 2). Each molecule is surrounded by six others in the same manner observed for **DBIC-2** (except with only two rings on each adjacent molecule overlapping in the edge-to-face orientation) via a shortest carbon−carbon distance of 3.7 Å, four of these in an edge-to-face arrangement and two in a completely offset parallel face-to-face arrangement. The crystal structures of **DBIC-1** and **DBIC-**
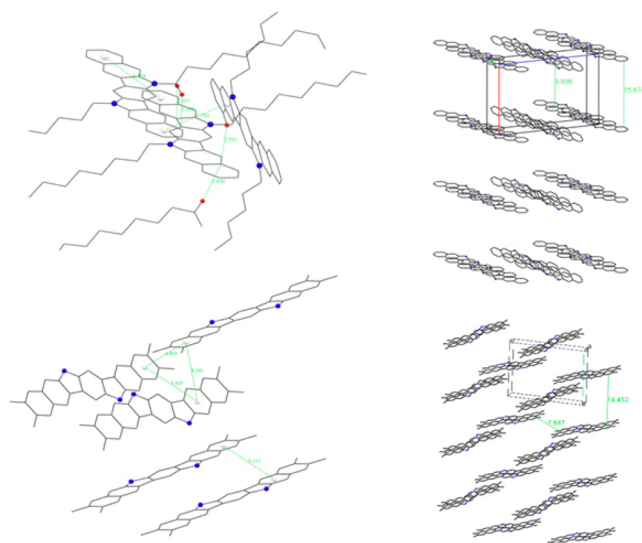
Figure 2. Crystal structures of **DBIC-2** (top) and **DBIC-3** (bottom).

2 show twisting of the alkyl chains, which implies that the packing structure is being dominated by the aromatic cores, with the alkyl chains twisting to accommodate the packing of the aromatic core.

DSC traces for compounds **DBIC-2** and **DBIC-3** both showed single melting point transitions at 194 and 229 °C, respectively. **DBIC-1**, with the longer branched alkyl chain, forms two mesophases, identified by polarized optical microscopy, that were observed at 100 and 104 °C before the material melted into an isotropic liquid at 106 °C.[14]

The HOMO energy levels of **DBIC-1** and **DBIC-2** suggest that devices should operate under ambient conditions (Table 1).[15] The introduction of methyl groups onto the backbone (**DBIC-3**) raises the HOMO energy level by 0.2 eV. All HOMO energy levels are raised relative to those reported for indolo[3,2-b]carbazoles in the literature and better match the work function of gold which should allow for effective charge injection (see Supporting Information (SI)). UV−vis spectroscopy showed an onset of absorption at around 515 nm for all three compounds, significantly red-shifted relative to indolo-[3,2-b]carbazoles ($\lambda_{onset} \approx 450$ nm)[1a] as a consequence of the extended conjugation length (see SI).

Preliminary OFET devices were fabricated by vacuum sublimation of **DBIC-2** and **DBIC-3** onto OTS treated SiO_2/Si^{++} wafers, while fabrication of devices based on **DBIC-1** was performed by spin coating from a 0.5% w/w solution in THF. **DBIC-1** and **DBIC-2** were found to show good transfer characteristics and similar mobilities of 2.6×10^{-3} and 4.0×10^{-3} ($\pm 1 \times 10^{-3}$) $cm^2 V^{-1} s^{-1}$, respectively, whereas **DBIC-3** exhibited a mobility 2 orders of magnitude lower (3.1×10^{-5}). This is possibly a consequence of the tighter crystal packing of **DBIC-2** relative to **DBIC-3**. Fabrication of devices based on **DBIC-2** using substrates maintained at 25 °C did not exhibit normal transfer characteristics making it difficult to obtain accurate values for the devices' performance. It was found that when a heated substrate (100 °C) was used during the evaporation, this problem was alleviated. Transfer and output curves for **DBIC-2** are shown in Figure 3.

Analysis by powder-XRD indicates that the orientation of **DBIC-2** on the two different temperature substrates is almost identical. A primary diffraction peak is observed at $2\theta = 5.70°$ (100 °C) (Figure 4) and 5.72° (25 °C), with second-, third-,

Table 1. Summary of Optical and Electronic Properties

	HOMO/ eV[a]	LUMO/ eV[b]	HOMO calcd[c]	LUMO calcd[c]	λ_{onset}/ nm	E_g/ eV	μ/cm^2 V s^{-1}	I_{on}/I_{off}	V_{th}	t/eV[c]	$\lambda_{(hole)}$/ eV[c]
DBIC-1	−5.13	−2.72	–	–	515	2.41	2.6×10^{-3} ($\pm 5 \times 10^{-4}$)[d]	1×10^3	−1	–	–
DBIC-2	−5.19	−2.79	−5.70	−0.77	516	2.40	4.0×10^{-3} ($\pm 1 \times 10^{-3}$)[e]	4×10^4	−19	0.11	0.076
DBIC-3	−4.99	−2.57	−5.52	−0.67	513	2.42	3.1×10^{-5} ($\pm 2.8 \times 10^{-5}$)[f]	4×10^3	−13	0.05	0.074

[a]Estimated from cyclic voltammetry using the equation: E_{HOMO} (eV) $= -(5.1 - E_{onset} + E_{1/2[Fc]})$. [b]Estimated from cyclic voltammetry (HOMO) and optical band gap. [c]See SI for computational method. [d]Fabricated by solution processing from THF (0.5% w/w solution) onto OTS−SiO$_2$. [e]Fabricated by vacuum evaporation onto OTS−SiO$_2$ at 100 °C. [f]Fabricated by vacuum evaporation onto OTS−SiO$_2$ at 25 °C.
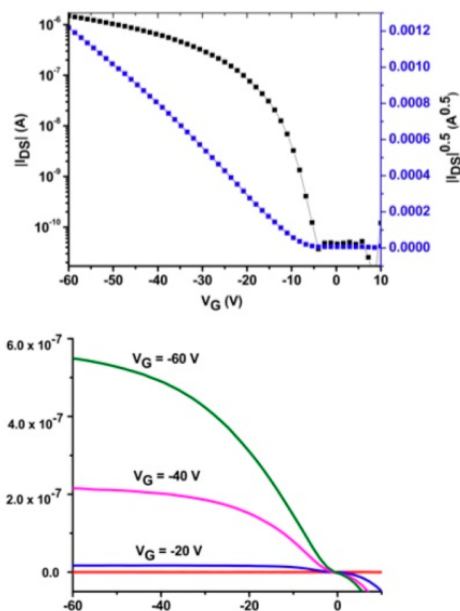

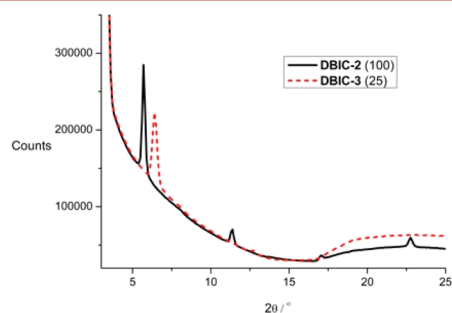**Figure 3.** Transfer (top) and output characteristics (bottom) for DBIC-2.

Figure 4. Powder-XRD for DBIC-2 and DBIC-3.

and fourth-order diffraction peaks visible in both cases. The primary diffraction peaks correspond to a *d*-spacing of 15.5 Å; this matches closely with the predicted (1,0,0) reflection from the single crystal data obtained, which gives a *d*-spacing of 15.7 Å. This hints that the compound may be adopting an orientation in which the alkyl chains are pointing both downward toward the substrate and upward away from the substrate, with the aromatic core laid with its longest axis off parallel by an angle of ∼35° relative to the substrate. **DBIC-3** displays a primary diffraction peak of 6.39°, corresponding to a *d*-spacing of 13.8 Å. This matches with the predicted primary diffraction peak at 6.56° (0,1,−1), estimated from the single crystal data, suggesting the aromatic core of the compound may be adopting a conformation with its long axis at an angle of ∼50° relative to the substrate. Using the coordinates from the

crystal structures, we estimated both transfer integrals (*t*) and reorganization energies (*λ*) for transport through **DBIC-2** and **DBIC-3**. Using semiclassical Marcus hopping theory, the rates of charge transfer (hole) were then calculated to be 0.22 and 0.02 s^{-1}.[16] The calculated reorganization energies are low and close in value (0.076 and 0.074 eV), with the source of the differing rates being derived from the large difference in the respective transfer integrals.

In summary, we have synthesized the previously unstudied dibenzoindolo[3,2-*b*]carbazoles by a novel, tag-assisted approach involving a two-directional Pummerer-type reaction and a two-directional SmI$_2$-mediated radical cascade. The use of a phase tag allows us to exploit intermediates that are unstable to purification by conventional chromatography and would otherwise need to be avoided. Dibenzoindolo[3,2-*b*]carbazoles show good ambient stability, with HOMO levels between −5.0 and −5.1 eV. The compounds were found to pack in a lamellar "herring bone-type" structure. Preliminary OFET devices were fabricated and found to provide modest mobilities of up to 4.0 × 10^{-3}. The optimization of device performance is currently underway in our laboratories.

■ ASSOCIATED CONTENT

Ⓢ Supporting Information

Experimental details for the preparation of compounds and devices, ^{1}H and ^{13}C NMR spectra for new compounds, DSC and CV traces. This material is available free of charge via the Internet at http://pubs.acs.org.

■ AUTHOR INFORMATION

Corresponding Author

*E-mail: david.j.procter@manchester.ac.uk.

Notes

The authors declare no competing financial interest.

■ ACKNOWLEDGMENTS

■ REFERENCES

(1) (a) Li, Y.; Wu, Y.; Gardner, S.; Ong, B. S. *Adv. Mater.* **2005**, *17*, 849. (b) Zhao, H.; Jiang, L.; Dong, H.; Li, H.; Hu, W.; Ong, B. S. *ChemPhysChem* **2009**, *10*, 2345. (c) Simokaitiene, J.; Stanislovaityte, E.; Grazulevicius, J. V.; Jankauskas, V.; Gu, R.; Dehaen, W.; Hung, Y.-C.; Hsu, C.-P. *J. Org. Chem.* **2012**, *77*, 4924. (d) Hu, N.-X.; Xie, S.; Popovic, Z. D.; Ong, B. S.; Hor, A.-M. *Synth. Met.* **2000**, 421. (e) Belletête, M.; Blouin, N.; Boudreault, P.-L. T.; Leclerc, M.; Durocher, G. *J. Phys. Chem. A* **2006**, *110*, 13696. (f) Li, Y.; Wu, Y.; Ong, B. S. *Macromolecules* **2006**, *39*, 6521. (g) Boudreault, P.-L. T.; Wakim, S.; Blouin, N.; Simard, M.; Tessier, C.; Tao, Y.; Leclerc, M. *J. Am. Chem. Soc.* **2007**, *129*, 9125. (h) Zhao, H.-P.; Tao, X.-T.; Wang,

P.; Ren, Y.; Yang, J.-X.; Yan, Y.-X.; Yuan, C.-X.; Liu, H.-J.; Zou, D.-C.; Jiang, M.-H. *Org. Electron.* **2007**, *8*, 673.

(2) (a) Anthony, J. E. *Chem. Rev.* **2006**, *106*, 5028. (b) Mondal, R.; Tönshoff, C.; Khon, D.; Neckers, D. C.; Bettinger, H. F. *J. Am. Chem. Soc.* **2009**, *131*, 14281. (c) Zade, S. S.; Bendikov, M. *Angew. Chem., Int. Ed.* **2010**, *49*, 4012. (d) Mondal, R.; Shah, B. K.; Neckers, D. C. *J. Am. Chem. Soc.* **2006**, *128*, 9612. (e) Watanabe, M.; Chang, Y. J.; Liu, S.-W.; Chao, T.-H.; Goto, K.; Islam, M. M.; Yuan, C.-H.; Tao, Y.-T.; Shinmyozu, T.; Chow, T. J. *Nat. Chem.* **2012**, *4*, 574.

(3) (a) Pho, T. V.; Yuen, J. D.; Kurzman, J. A.; Smith, B. G.; Miao, M.; Walker, W. T.; Seshadri, R.; Wudl, F. *J. Am. Chem. Soc.* **2012**, *134*, 18185. (b) De, P. K.; Neckers, D. C. *Org. Lett.* **2012**, *14*, 78. (c) Kaur, I.; Stein, N. N.; Kopreski, R. P.; Miller, G. P. *J. Am. Chem. Soc.* **2009**, *131*, 3424. (d) Chun, D.; Cheng, Y.; Wudl, F. *Angew. Chem., Int. Ed.* **2008**, *47*, 8380. (e) Ye, Q.; Chang, J.; Huang, K.-W.; Dai, G.; Zhang, J.; Chen, Z.-K.; Wu, J.; Chi, C. *Org. Lett.* **2012**, *14*, 2786. (f) Balaji, G.; Della Pelle, A. M.; Popere, B. C.; Chandrasekaran, A.; Thayumanavan, S. *Org. Biomol. Chem.* **2012**, *10*, 3455. (g) Qu, H.; Chi, C. *Org. Lett.* **2010**, *12*, 3360. (h) Payne, M. M.; Parkin, S. R.; Anthony, J. E. *J. Am. Chem. Soc.* **2005**, *127*, 8028.

(4) For a review of the Pummerer reaction, see: Smith, L. H. S.; Coote, S. C.; Sneddon, H. F.; Procter, D. J. *Angew. Chem., Int. Ed.* **2010**, *49*, 5832.

(5) For a recent review, see: (a) Szostak, M.; Spain, M.; Procter, D. J. *Chem. Soc. Rev.* **2013**, *42*, 9155. (b) Szostak, M.; Procter, D. J. *Angew. Chem., Int. Ed.* **2012**, *51*, 9238. (c) Procter, D. J.; Flowers, R. A., II; Skrydstrup, T. *Organic Synthesis Using Samarium Diiodide: A Practical Guide* RSC Publishing: Cambridge, 2010.

(6) (a) McAllister, L. A.; McCormick, R. A.; Brand, S.; Procter, D. J. *Angew. Chem., Int. Ed.* **2005**, *44*, 452. (b) McAllister, L. A.; McCormick, R. A.; James, K. M.; Brand, S.; Willetts, N.; Procter, D. J. *Chem.—Eur. J.* **2007**, *13*, 1032. (c) James, K. M.; Willetts, N.; Procter, D. J. *Org. Lett.* **2008**, *10*, 1203. (d) Coote, S. C.; Quenum, S.; Procter, D. J. *Org. Biomol. Chem.* **2011**, *9*, 5104.

(7) (a) Miller, M.; Tsang, W.; Merritt, A.; Procter, D. J. *Chem. Commun.* **2007**, 498. (b) Ovens, C.; Martin, N. G.; Procter, D. J. *Org. Lett.* **2008**, *10*, 1441. (c) Miller, M.; Vogel, J. C.; Tsang, W.; Merritt, A.; Procter, D. J. *Org. Biomol. Chem.* **2009**, *7*, 589. (d) Smith, L. H. S.; Nguyen, T. T.; Sneddon, H. F.; Procter, D. J. *Chem. Commun.* **2011**, *47*, 10821. (e) Ovens, C.; Vogel, J. C.; Martin, N. G.; Procter, D. J. *Chem. Commun.* **2009**, 3101.

(8) (a) Rumer, J. W.; Dai, S.-Y.; Levick, M.; Biniek, L.; Procter, D. J.; McCulloch, I. *J. Polym. Sci., Part A: Polym. Chem.* **2013**, *51*, 1285. (b) Rumer, J. W.; Dai, S.-Y.; Levick, M.; Kim, Y.; Madec, M.-B.; Ashraf, R. S.; Huang, Z.; Rossbauer, S.; Schroeder, B.; Biniek, L.; Watkins, S. E.; Anthopoulos, T. D.; Janssen, R. A. J.; Durrant, J. R.; Procter, D. J.; McCulloch, I. *J. Mater. Chem. C* **2013**, *1*, 2711. (c) Rumer, J. W.; Levick, M.; Dai, S.-Y.; Rossbauer, S.; Huang, Z.; Biniek, L.; Anthopoulos, T. D.; Durrant, J. R.; Procter, D. J.; McCulloch, I. *Chem. Commun.* **2013**, *49*, 4465.

(9) Levick, M. T.; Coote, S. C.; Grace, I.; Lambert, C.; Turner, M. L.; Procter, D. J. *Org. Lett.* **2012**, *14*, 5744.

(10) For a discussion of fluorous tagging, see: (a) Studer, A.; Hadida, S.; Ferritto, R.; Kim, S.-Y.; Jeger, P.; Wipf, P.; Curran, D. P. *Science* **1997**, *275*, 823. For a review, see: (b) Curran, D. P. In *The Handbook of Fluorous Chemistry*; Gladysz, J. A., Curran, D. P., Horvath, I. T., Eds.; Wiley-VCH: Weinheim, 2004.

(11) (a) Curran, D. P.; Luo, Z. *J. Am. Chem. Soc.* **1999**, *121*, 9069. (b) Zhang, W.; Curran, D. P. *Tetrahedron* **2006**, *62*, 11837.

(12) For SmI_2-mediated linker cleavage, see: (a) McAllister, L. A.; Brand, S.; de Gentile, R.; Procter, D. J. *Chem. Commun.* **2003**, 2380. (b) Turner, K. L.; Baker, T. M.; Islam, S.; Procter, D. J.; Stefaniak, M. *Org. Lett.* **2006**, *8*, 329. (c) McAllister, L. A.; Turner, K. L.; Brand, S.; Stefaniak, M.; Procter, D. J. *J. Org. Chem.* **2006**, *71*, 6497. (d) McKerlie, F.; Procter, D. J.; Wynne, G. *Chem. Commun.* **2002**, 584. (e) McKerlie, F.; Rudkin, I. M.; Wynne, G.; Procter, D. J. *Org. Biomol. Chem.* **2005**, *3*, 2805. (f) For a review on sulfur and selenium linkers in phase tag-assisted synthesis, see: McAllister, L. A.; McCormick, R. A.; Procter, D. J. *Tetrahedron* **2005**, *61*, 11527.

(13) See SI for CCDC numbers.

(14) These mesophases both displayed the 'mosaic' texture characteristic of the soft crystal or hexatic liquid crystal phases (see SI). Dierking, I. *Textures of Liquid Crystals*; Wiley-VCH: Weinheim, 2003; Chapters 9–10.

(15) Cardona, C. M.; Li, W.; Kaifer, A. E.; Stockdale, D.; Bazan, G. C. *Adv. Mater.* **2011**, *23*, 2367.

(16) Koh, S. E.; Risko, C.; da Silva Filho, D. A.; Kwon, O.; Facchetti, A.; Brédas, J.-L.; Marks, T. J.; Ratner, M. A. *Adv. Funct. Mater.* **2008**, *18*, 332.